GEOPHYSICAL RESEARCH LETTERS, VOL. 35, L19111, doi:10.1029/2008GL035454, 2008



# Intermittent MHD structures and classical discontinuities

A. Greco,[1,2] P. Chuychai,[1] W. H. Matthaeus,[1] S. Servidio,[1] and P. Dmitruk[3]

Received 23 July 2008; accepted 5 September 2008; published 15 October 2008.

[1] We examine statistics of rapid spatial variations of the magnetic field in simulations of magnetohydrodynamic (MHD) turbulence, by analyzing intermittency properties, and by using classical methods for identifying discontinuities. The methods identify similar structures, and give very similar event distribution functions. When the results are scaled to the correlation length, the average waiting times agree with typically reported waiting times between solar wind discontinuities. Thus discontinuities may be related to flux tube boundaries and intermittent structures that appear spontaneously in MHD turbulence. **Citation:** Greco, A., P. Chuychai, W. H. Matthaeus, S. Servidio, and P. Dmitruk (2008), Intermittent MHD structures and classical discontinuities, *Geophys. Res. Lett.*, *35*, L19111, doi:10.1029/2008GL035454.

## 1. Introduction

[2] There are numerous directional discontinuities (DDs) in the interplanetary magnetic field [*Ness et al.*, 1966] on the time scale of seconds. Many studies identify these as statically advected tangential (TDs) or propagating rotational (RDs) discontinuities [*Tsurutani and Smith*, 1979; *Lepping and Behannon*, 1986; *Knetter et al.*, 2004; *Neugebauer et al.*, 1984; *Vasquez et al.*, 2007]. There is still debate regarding the relative frequency [*Neugebauer*, 2006], and the origin [*Vasquez et al.*, 2007] of these structures. Both types of discontinuities are classically viewed as special persistent solutions to the MHD equations. In this Letter we explore an alternative possibility, that observed discontinuities might not be static solutions to the MHD equations, but instead might be associated with turbulence. Our approach is to compare statistical properties of discontinuities, as measured using classical methods, with intermittency properties of MHD turbulence.

[3] There are ambiguities in identification of TDs and RDs, and differences in the defining criteria [*Burlaga*, 1969; *Tsurutani and Smith*, 1979; *Lepping and Behannon*, 1986; *Li*, 2008]. There are also differences in interpretation: one familiar view is that discontinuities are static boundaries between flux tubes originating in the lower corona (or photosphere). For example, TDs may be persistent current sheets bounding convected flux tubes [*Parker*, 1994]. In this "spaghetti" view, the tubes may tangle up in space, but remain distinct entities [e.g., see *Bruno et al.*, 2001], with different magnetic field, density, temperature, etc. Within each flux tube the presence of Alfvénic fluctuations causes random wandering about the main flux tube magnetic field. Closely related is the view that solar wind fluctuations are a superposition of propagating Alfvén waves and convected structures [*Bavassano and Bruno*, 1989; *Tu and Marsch*, 1993]. An alternative hypothesis examined here is that observed discontinuities are small scale coherent structures that emerge in fully developed intermittent MHD turbulence [*Matthaeus and Lamkin*, 1986; *Veltri*, 1999]. In particular, coherent current sheets form between flux tubes, and a subset of these might involve magnetic reconnection [*Dmitruk and Matthaeus*, 2006]. These coherent structures can appear in less than one nonlinear time beginning from Gaussian initial data that completely lack coherent structures [*Servidio et al.*, 2008]. Phase-correlated coherent structures imply intermittency, which has been studied in MHD theory, simulations and in the solar wind [*Carbone et al.*, 1990; *Burlaga*, 1991; *Horbury and Balogh*, 1997; *Tu et al.*, 1996; *Sorriso-Valvo et al.*, 1999, 2000; *Li*, 2008]. MHD turbulence thus motivates examination of the possible link between observed discontinuities and turbulent dynamics.

## 2. Simulation and Analysis Procedure

[4] To study discontinuities, we use a Fourier pseudo-spectral method compressible Hall MHD code [*Dmitruk and Matthaeus*, 2006] in a periodic box of side $L = 2\pi L_0$. The spatial resolution is $256^3$ grid points. To make contact with the solar wind, we consider simulations with $\beta = 1$, correlation length $\lambda_c \ll L$, and large mean field. The Alfvénic Mach number is = 1, and equal dimensionless resistivity and viscosity = 1/1000. The magnetic Reynolds number is $R_m = 1000$. The mean magnetic field is $\mathbf{B}_0 = 4\,\hat{x}$. Initial energy spectra are flat out to a "bendover scale" $k_{bend} \sim 8$, above which the spectrum steepens. This gives $\lambda_c = 2\pi L_0/8$ and initial dissipation wavenumber $k_{diss} \sim 100$. The Hall (ion inertial) scale $k_H^{-1}$ is set so that $k_{diss}/k_H \sim 3$ as in the solar wind. We report on representative results at $t = 0.5t_A$ ($t_A$ is the Alfvén time), when the energy dissipation is near its peak value.

[5] With a strong $B_0$, turbulence develops anisotropy with stronger gradients perpendicular to the mean field and weaker parallel gradients [*Oughton et al.*, 1994]. Figure 1 illustrates one component of current density, $J_x$ (along $\mathbf{B}_0$) in a portion of the cube. $J_x$ is an intermittent quantity-there are large regions of small $J_x$, and large $J_x$ values are found in smaller spatial regions.

[6] To emulate spacecraft data, we sample the magnetic field **B**, current density **J**, velocity **v**, and density $\rho$ along a linear path through the simulation domain. When the trajectory leaves the box, it returns periodically to another side. To avoid spurious periodicity effects, the trajectory makes an angle relative to the axes of the box. Thus, upon re-entry, it is displaced from the initial trajectory by a

[1]Bartol Research Institute, University of Delaware, Newark, Delaware, USA.
[2]Department of Physics, University of Calabria, Rende, Italy.
[3]Departamento de Física, Universidad de Buenos Aires, Buenos Aires, Argentina.


0094-8276/08/2008GL035454$05.00

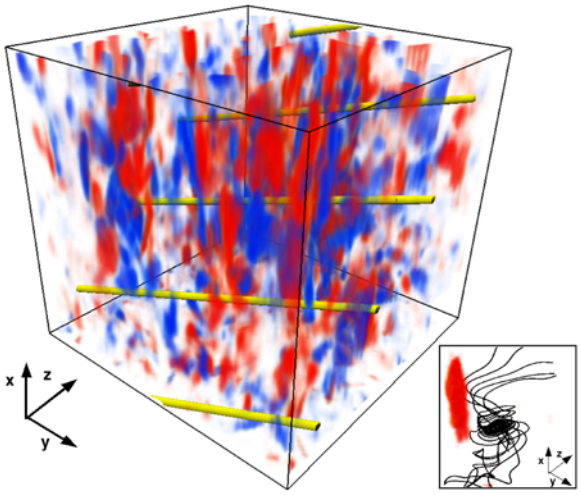


**Figure 1.** 3D view of current density $J_x$ in a portion of the simulation box (Red, $J_x > 0$; blue, $J_x < 0$). Solid yellow lines are sample trajectories. The inset shows an example of helical magnetic field lines (black) suggesting a flux tube, bounded by a current sheet (red).

correlation scale or more. This procedure can continue for a number of re-entries, producing a sample trajectory much longer than the box side. The trajectory direction $\hat{s}$, is determined by

$$\phi > \tan^{-1}\left(\frac{\lambda_c}{L}\right) \text{ and } \alpha > \tan^{-1}\left(\frac{\lambda_c}{\sqrt{(L^2+\lambda_c^2)}}\right), \qquad (1)$$

where $\phi$ and $\alpha$ are the angles between $\hat{s}$ and two Cartesian directions $\hat{x}$ and $\hat{y}$ that define the box. This minimizes periodicity effects while substantially increasing the statistical weight. The samples along the trajectory are separated by $2\Delta x$; $\Delta x = 2\pi/256$ is the grid size. We obtain **B**, **J**, **v** and $\rho$ at those positions by linear interpolation. Figure 1 illustrates a sample trajectory, which intersects small scale current structures.

## 3. Intermittency and Discontinuities

[7] In order to associate discontinuities with these small intermittent structures, we analyze the series of the magnitude of the magnetic field vector increments $|\Delta_{\Delta s}\mathbf{B}| = |\mathbf{B}(s + \Delta s) - \mathbf{B}(s)|$ at points separated by $\Delta s$ as is done in standard methods [*Tsurutani and Smith*, 1979]. (To simplify notation we suppress the parameter $\Delta s$ except where needed for clarity.) We examine two well separated scales: $\Delta s = 2\Delta x = 0.0625\lambda_c$, corresponding roughly to the boundary between the dissipation and inertial ranges and $\Delta s = 81\Delta x = 2.53\lambda_c$, a scale lying in the energy range. In Figure 2a, we show the Probability Density Functions (PDFs) of the $x$ component $\Delta\mathbf{B}_x$ calculated at separations $\Delta s = 2\Delta x$ and at $\Delta s = 81\Delta x$. The PDFs are computed as constant statistical weight densities [*Padhye et al.*, 2001]. The $2\Delta x$ PDF is very similar to the PDF of a component of current density, $J_y$, also shown in Figure 2a. The close correspondence of the PDFs of $\Delta\mathbf{B}_x$ and $J_y$ at separation $\Delta s = 2\Delta x$ is significant because one point spacecraft measurements cannot measure current, but can measure magnetic increments. Because of this statistical correspondence, we may be able to identify some "events" using increments and link these to current sheet structures which have similar intermittency properties. From Figure 2a we can conclude that the increments at large separation $\Delta s = 81\Delta x$ are almost Gaussian (see Gaussian curve for comparison) while increments at small scales $\Delta s = 2\Delta x$ display strong non Gaussian tails, indicating intermittency.

[8] Figure 2b compares the PDFs of $|\Delta\mathbf{B}|$ computed for inertial range $2\Delta x$, and energy range $81\Delta x$ separations. As expected $|\Delta\mathbf{B}|$ at large separations again compares well to the Gaussian case (also shown), while at small separations $2\Delta x$ there is a range, $|\Delta\mathbf{B}| \sim 2\Sigma$ or greater, in which non-Gaussian features are seen distinctly. Almost all events occurring above $2\Sigma$ are associated with non-Gaussian features. Consequently, in this range we can select "events" which, in turn, evidence the presence of intermittency.

[9] Besides the standard statistical measure $|\Delta\mathbf{B}|$, we compute another time series which is related to intermittency measure and that may better describe the events identified above, that is the normalized partial variance of increments (PVI)

$$\Im^{(2)} = \frac{|\Delta\mathbf{B}|^2}{\Sigma^2} \qquad (2)$$

where $\Sigma^2 = \langle|\Delta\mathbf{B}|^2\rangle$. In Figure 3, PVI is shown vs the distance $s$, normalized to the correlation length, along a sample trajectory (as in Figure 1) on the more intermittent scale $\Delta s = 2\Delta x$. Note that the PVI timeseries has the properties that its mean value is unity by construction. However, the non-central second moment of PVI is related to the kurtosis of the increments, thus establishing a quantitative connection between large variations of PVI and the intermittency of the turbulence. To make a practical verification of the latter point, we choose a threshold value of PVI (as shown, e.g., at the bottom of Figure 3), and all events above this threshold are excluded. Then, we calculate the kurtosis of the remaining signal. This is repeated with

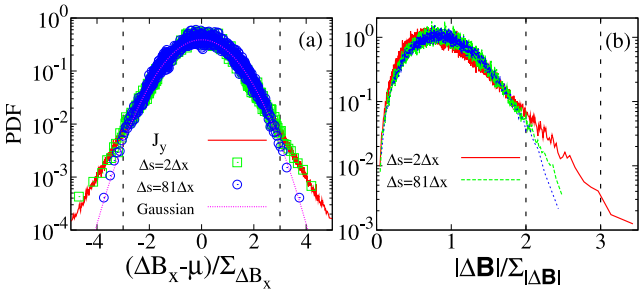


**Figure 2.** (a) PDF of $(\Delta B_x - \mu)/\Sigma_{\Delta Bx}$ ($\mu$ the average and $\Sigma_{\Delta Bx}$ the standard deviation of $\Delta B_x$) computed at separations $\Delta s = 2\Delta x$ and $81\Delta x$, and PDF of $(J_y - \langle J_y\rangle)/\Sigma_{Jy}$ ($\langle J_y\rangle$ the average and $\Sigma_{Jy}$ the standard deviation of $J_y$). (b) PDF of $|\Delta\mathbf{B}|/\Sigma_{|\Delta\mathbf{B}|}$, $(\Sigma_{|\Delta\mathbf{B}|} = \langle|\Delta\mathbf{B}|^2\rangle^{1/2})$ for the same two values of $\Delta s$. Dotted curves are PDF of one component of a random vector **A** having unit variance and independent Gaussian distributions (Figure 2a) and PDF of the modulus $|\mathbf{A}|$ (Figure 2b).

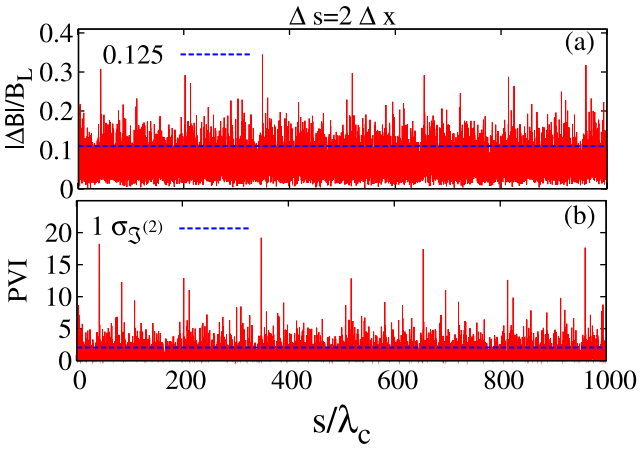


**Figure 3.** (a) $|\Delta\mathbf{B}|/B_L$, and (b) PVI vs the distance $s/\lambda_c$ on $\Delta s = 2\Delta x$. The dashed lines are the values of the thresholds (see the text). We plot only a portion of the entire data set.

varying values of the threshold until the kurtosis of the remaining signal is equal to the value expected for the squared modulus of a random vector having independent, Gaussian distributed components. After this procedure, we find that a suitable value of the threshold to use in subsequent analysis is $\langle \Im^{(2)} \rangle + \sigma_{\Im(2)}$ where $\sigma_{\Im(2)}$ is the noncentral standard deviation of PVI. Using the normalization of PVI given in equation (2), this threshold has a value ≈2.4. For this threshold value, we verify that selected "spikes" are related to the intermittent character of the signal.

[10] The present hypothesis is that the statistics of intermittent events calculated in this way might be related to the statistics implemented in classical methods for identifying MHD discontinuities [*Tsurutani and Smith*, 1979] in solar wind studies (hereafter TS). To affect this comparison we continue to use a separation of $\Delta s = 2\Delta x$ and the same simulation data as above. The first requirement in the TS methodology is that the magnitude of the magnetic vector change over distance $\Delta s$ across the discontinuity must exceed $B_L/2$ where $B_L$ is the larger of the field magnitudes on either side of the discontinuity. Related methods use a similar first-level criterion. Figure 3 illustrates the time series $|\Delta\mathbf{B}|/B_L$ computed from the simulation, where it can be compared with the PVI time series from the same data.

[11] The second TS requirement checks whether the vector jump is large in comparison with the level of fluctuations in the vicinity of discontinuity, measured by a local variance of $|\Delta\mathbf{B}|$ (say, $\delta^2$) computed from 5 values in the neighborhood of each point in the time series. According to these criteria, the selected events that are identified as discontinuities are relatively major features that stand out against the background fluctuations.

[12] Following the TS method, we put two thresholds on the $|\Delta\mathbf{B}|$ simulation time series, which is shown in the top panel of Figure 3. The actual value used is normalized to the value of the mean magnetic field $B_0 = 4$. We compute the second TS threshold as $|\Delta\mathbf{B}| > 2\delta$; the corresponding series is not shown here. Using this implementation of the TS method, we compute a series of discontinuities, or events, from the MHD simulation.

[13] We now compare event identification using the TS and PVI methods. First, we compute the probability density function of the waiting time (or distance) between the events [*Tsurutani and Smith*, 1979; *Burlaga*, 1969; *Bruno et al.*, 2001; *Vasquez et al.*, 2007] in each set of data. The waiting time measures the elapsed time between the end of an event and the beginning of the next one, and is a familiar and useful statistical tool in space physics, astrophysics and other fields. Here we examine whether the probability distributions of the waiting times in simulations support a possible link between the MHD intermittency and solar wind discontinuities. We defer direct comparison to solar wind statistics to a later publication.

[14] In Figure 4, we show the PDFs of the waiting distance $s$, normalized to the correlation length $\lambda_c$, for the events selected from the PVI time series and for the discontinuities determined by our implementation of the TS method. The two distributions are remarkably similar, suggesting that the performance of the two methods is comparable. In fact, many of the events selected by the two methods are the same. The correlation coefficient between PVI events and the TS events is 0.87. Evidently, the TS method, designed to detect MHD discontinuities, is effective in identifying intermittency of MHD turbulence.

## 4. Conclusions

[15] Through analysis of Hall MHD simulation data, we have examined the relationship between discontinuities identified by classical (TS) methods, and coherent structures identified using (PVI) intermittency statistics. The main differences in the methods are in the normalization of the time series ($B_L$ vs. $\Sigma$ normalizations), and in the use of two criteria in the TS method. The PVI method is directly connected to the presence of non-Gaussian features, and so is conceptually related to intermittency. The two methods produce remarkably similar distributions of waiting times, and in fact identify many of the same events. The distributions for $s < \lambda_c$ are well fit by a power law $\sim s^{-0.92}$, and by an exponential for $s > \lambda_c$.

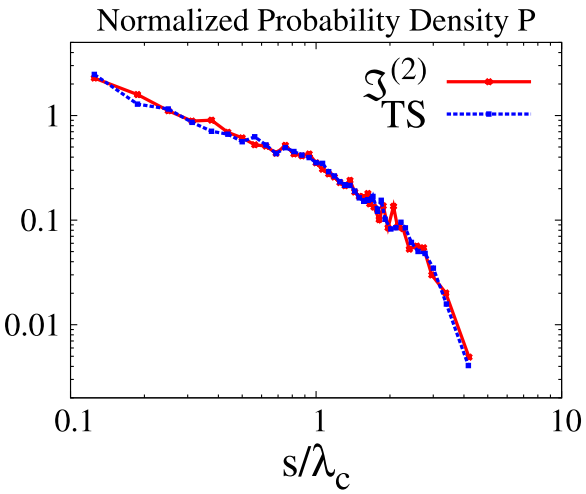


**Figure 4.** PDFs of the waiting "distance" $s$ normalized to the correlation length $\lambda_c$ for the time series of PVI and for the discontinuities selected from the time series $|\Delta\mathbf{B}|$ applying the Tsurutani and Smith method. The axes are in log-log scale.

[16] It is instructive to make a preliminary comparison of waiting times in the simulations, and published solar wind results. The average waiting distance computed directly from the PDFs is $\sim 0.8\lambda_c$ for both simulation data sets (see Figure 4). We compare this value to reported solar wind waiting times for discontinuities identified using standard methods. Let us assume that correlation length $\lambda_c$ in the solar wind is $1.2 \times 10^6$ km and that discontinuities convect past the spacecraft at $\sim$400 km/s. Then a mean waiting distance of 1 $\lambda_c$, as we found above, corresponds in the solar wind to an average waiting time $\sim$50 min. This result does not disagree greatly with previous analysis performed by *Tsurutani and Smith* [1979], who found that at 1 AU the average waiting time of 14 min, where the discontinuity identification was carried out with a time separation of $\Delta t$ = 3 min. (This is approximately equivalent, to a separation of $\Delta s = 2\Delta x$ using $\Delta t = \Delta s/V_{sw}$ and normalizing lengths to $\lambda_c$.) TS also remark that their average wait time may be better quantified as 2 discontinuities per hour (30 min waiting time) when very closely spaced events are taken in to account. The present result is also in good agreement with the finding of *Bruno et al.* [2001] of an average waiting time of about 33 min.

[17] The hypothesis that some (or most) solar wind discontinuities are consequences of intermittent turbulence is supported by the present results. Further study is needed to distinguish what fraction of near-discontinuous solar wind events emerge from in-situ turbulence processes [*Vasquez et al.*, 2007], and what fraction convect passively from solar source regions. In turbulence current sheets bound interacting flux tubes, and some of these may be involved in reconnection [*Dmitruk and Matthaeus*, 2006; *Servidio et al.*, 2008]. The present approach might help to identify local turbulent reconnection sites [*Gosling et al.*, 2007] of the type seen in the magnetosheath [*Retinò et al.*, 2007]. We also cannot rule out that signatures of intermittency originate in the corona. Further studies will clarify these connections between classical methods and intermittency analysis.

[18] **Acknowledgments.** Supported in part by NASA Heliophysics Theory NNX08AI47G, NSF ATM-0539995 and SHINE ATM-0752135. We use NCAR Vapor graphics software (www.vapor.ucar.edu).

## References

Bavassano, B., and R. Bruno (1989), Large-scale solar wind fluctuations in the inner heliosphere at low solar activity, *J. Geophys. Res.*, *94*, 168–176.

Bruno, R., V. Carbone, P. Veltri, E. Pietropaolo, and B. Bavassano (2001), Identifying intermittency events in the solar wind, *Planet. Space Sci.*, *49*, 1201–1210.

Burlaga, L. F. (1969), Directional discontinuities in the interplanetary magnetic field, *Sol. Phys.*, *7*, 54–71.

Burlaga, L. F. (1991), Intermittent turbulence in the solar wind, *J. Geophys. Res.*, *96*, 5847–5851.

Carbone, V., P. Veltri, and A. Mangeney (1990), Coherent structure formation and magnetic field line reconnection in magnetohydrodynamic turbulence, *Phys. Fluids*, *2*, 1487–1496.

Dmitruk, P., and W. H. Matthaeus (2006), Structure of the electromagnetic field in three-dimensional Hall magnetohydrodynamic turbulence, *Phys. Plasmas*, *13*, 112303.

Gosling, J. T., T. D. Phan, R. P. Lin, and A. Szabo (2007), Prevalence of magnetic reconnection at small field shear angles in the solar wind, *Geophys. Res. Lett.*, *34*, L15110, doi:10.1029/2007GL030706.

Horbury, T. S., and A. Balogh (1997), Structure function measurements of the intermittent MHD turbulent cascade, *Nonlinear Processes Geophys.*, *4*, 185–199.

Knetter, T., F. M. Neubauer, T. Horbury, and A. Balogh (2004), Four-point discontinuity observations using Cluster magnetic field data: A statistical survey, *J. Geophys. Res.*, *109*, A06102, doi:10.1029/2003JA010099.

Lepping, R. P., and K. W. Behannon (1986), Magnetic field directional discontinuities: Characteristics between 0.46 and 1.0 AU, *J. Geophys. Res.*, *91*, 8725–8741.

Li, G. (2008), Identifying current-sheet-like structures in the solar wind, *Astrophys. J.*, *672*, L65–L68.

Matthaeus, W. H., and S. L. Lamkin (1986), Turbulent magnetic reconnection, *Phys. Fluids*, *29*, 2513–2534.

Ness, N. F., C. S. Scearce, and S. Cantarano (1966), Preliminary results from Pioneer 6 magnetic field experiment, *J. Geophys. Res.*, *71*, 3305–3313.

Neugebauer, M. (2006), Comment on the abundances of rotational and tangential discontinuities in the solar wind, *J. Geophys. Res.*, *111*, A04103, doi:10.1029/2005JA011497.

Neugebauer, M., D. R. Clay, B. E. Goldstein, B. T. Tsurutani, and R. D. Zwickl (1984), A reexamination of rotational and tangential discontinuities in the solar wind, *J. Geophys. Res.*, *89*, 5395–5408.

Oughton, S., E. R. Priest, and W. H. Matthaeus (1994), The influence of a mean magnetic field on three-dimensional magnetohydrodynamic turbulence, *J. Fluid Mech.*, *280*, 95–117.

Padhye, N. S., C. W. Smith, and W. H. Matthaeus (2001), Distribution of magnetic field components in the solar wind plasma, *J. Geophys. Res.*, *106*, 18,635–18,650.

Parker, E. N. (1994), *Spontaneous Current Sheets in Magnetic Fields With Applications to Stellar X-Rays*, Oxford Univ. Press, New York.

Retinò, A., D. Sundkvist, A. Vaivads, F. Mozer, M. André, and C. J. Owen (2007), In situ evidence of magnetic reconnection in turbulent plasma, *Nature Phys.*, *3*, 236–238.

Servidio, S., W. H. Matthaeus, and P. Dmitruk (2008), Depression of nonlinearity in decaying isotropic MHD turbulence, *Phys. Rev. Lett.*, *100*, 095005.

Sorriso-Valvo, L., V. Carbone, P. Veltri, G. Consolini, and R. Bruno (1999), Intermittency in the solar wind turbulence through probability distribution functions of fluctuations, *Geophys. Res. Lett.*, *26*, 1801–1804.

Sorriso-Valvo, L., V. Carbone, P. Veltri, H. Politano, and A. Pouquet (2000), Non-Gaussian probability distribution functions in two dimensional magnetohydrodynamic turbulence, *Europhys. Lett.*, *51*, 520–526.

Tsurutani, B. T., and E. J. Smith (1979), Interplanetary discontinuities: Temporal variations and the radial gradient from 1 to 8.5 AU, *J. Geophys. Res.*, *84*, 2773–2787.

Tu, C.-Y., and E. Marsch (1993), A model of solar wind fluctuations with two components: Alfvén waves and convective structures, *J. Geophys. Res.*, *98*, 1257–1276.

Tu, A.-Y., E. Marsch, and H. Rosenbauer (1996), An extended structure-function model and its application to the analysis of solar wind intermittency properties, *Ann. Geophys.*, *14*, 270–285.

Vasquez, B. J., V. I. Abramenko, D. K. Haggerty, and C. W. Smith (2007), Numerous small magnetic field discontinuities of Bartels rotation 2286 and the potential role of Alfvénic turbulence, *J. Geophys. Res.*, *112*, A11102, doi:10.1029/2007JA012504.

Veltri, P. (1999), MHD turbulence in the solar wind: Self-similarity, intermitency, coherent structures, *Plasma Phys. Controlled Fusion*, *41*, 787–795.

P. Chuychai, A. Greco, W. H. Matthaeus, and S. Servidio, Bartol Research Institute, University of Delaware, Newark, DE 19716, USA. (whm@udel.edu)

P. Dmitruk, Departamento de Física, Universidad de Buenos Aires, 1428 Buenos Aires, Argentina.